Published in final edited form as:
J Biol Chem. 2003 July 18; 278(29): 27208–27215. doi:10.1074/jbc.M301118200.

Caveolin-1 Contributes to Assembly of Store-operated Ca^{2+} Influx Channels by Regulating Plasma Membrane Localization of TRPC1

So-ching W. Brazer,
Secretory Physiology Section, Gene Therapy and Therapeutics Branch, NIDCR, National Institutes of Health, Bethesda, Maryland 20892

Brij B. Singh,
Secretory Physiology Section, Gene Therapy and Therapeutics Branch, NIDCR, National Institutes of Health, Bethesda, Maryland 20892

Xibao Liu,
Secretory Physiology Section, Gene Therapy and Therapeutics Branch, NIDCR, National Institutes of Health, Bethesda, Maryland 20892

William Swaim, and
Cellular Imaging Core, Department of Health and Human Services, NIDCR, National Institutes of Health, Bethesda, Maryland 20892

Indu S. Ambudkar[§]
Secretory Physiology Section, Gene Therapy and Therapeutics Branch, NIDCR, National Institutes of Health, Bethesda, Maryland 20892

Abstract

TRPC1, a component of store-operated Ca^{2+} entry (SOCE) channels, is assembled in a complex with caveolin- 1 (Cav1) and key Ca^{2+} signaling proteins. This study examines the role of Cav1 in the function of TRPC1. TRPC1 and Cav1 were colocalized in the plasma membrane region of human submandibular gland and Madin-Darby canine kidney cells. Full-length Cav1 bound to both the N and C termini of TRPC1. Amino acids 271–349, which includes a Cav1 binding motif (amino acids 322–349), was identified as the Cav1 binding domain in the TRPC1 N terminus. Deletion of amino acids 271–349 or 322–349 prevented plasma membrane localization of TRPC1. Importantly, TRPC1Δ271–349 induced a dominant suppression of SOCE and was associated with wild-type TRPC1. Although the role of the C-terminal Cav1 binding domain is not known, its deletion did not affect localization of TRPC1 (Singh, B. B., Liu, X., and Ambudkar, I. S. (2000) *J. Biol. Chem.* 275, 36483–36486). Further, expression of a truncated Cav1 (Cav1Δ51–169), but not full-length Cav1, similarly disrupted plasma membrane localization of endogenously and exogenously expressed TRPC1 in human Submandibular gland and Madin-Darby canine kidney cells. Cav1Δ51–169 also suppressed thapsigargin- and carbachol-stimulated Ca^{2+} influx and increased the detergent solubility of TRPC1, although plasma membrane lipid raft domains were not disrupted. These data demonstrate that plasma membrane localization of TRPC1 depends on an interaction between its N terminus and Cav1. Thus, our data suggest that Cav1 has an important role in the assembly of SOCE channel(s).

[§]To whom correspondence should be addressed: Bldg. 10, Rm. 1N-113, National Institutes of Health, Bethesda, MD 20892. Tel.: 301-496-5298; Fax: 301-402-1228; indu.ambudkar@nih.gov.

SOCE[1] is activated in response to stimulation of plasma membrane receptors that are coupled to the mobilization of intracellular Ca^{2+}. Although there is considerable evidence to suggest that the signal for the activation of SOCE is the depletion of Ca^{2+} within the endoplasmic reticulum (1), the mechanism involved in activation or inactivation of SOCE is not yet known. A major drawback in understanding the mechanism of SOCE has been the lack of information regarding the identity and regulation of the SOCE channel. Members of the TRPC protein family have been suggested as molecular components of the SOCE channel (2–4). TRPC1 has been reported to be required for SOCE in several cell types (5–8). Our previous studies showed that TRPC1 is a critical component of SOCE in salivary epithelial cells (9–11). Further, we reported previously that, like the *Drosophila* TRP (12), TRPC1 and TRPC3 are assembled in signaling complexes that are associated with Cav1 and key Ca^{2+} signaling proteins such as $G\alpha_{q/11}$, inositol trisphosphate receptor, phospholipase Cβ, PMCA (plasma membrane Ca^{2+} pump), SERCA (sarco-endoplasmic reticulum Ca^{2+} pump), and calmodulin (13–15). The *Drosophila* TRP signalplex is assembled via INAD, a multi-PDZ domain-containing protein. INAD binds to a number of proteins in the complex and determines its localization in the rhabdomeres (4, 12). Interestingly, the components of this signalplex appear to be trafficked independently to the plasma membrane, and interaction with INAD is required for their retention at that location. Although several mammalian PDZ domain-containing proteins have been shown to act as scaffolds for receptor-associated signaling complexes in the plasma membrane (16), little is known about the organization of TRPC channels in mammalian cells (17). Tang *et al.* (18) have reported that NHERF, a two PDZ domain-containing protein that associates with the actin cytoskeleton via interactions with members of ezrin/radixin/moesin family, also interacts with TRPC4 and TRPC5 and might be involved in their association with phospholipase C isozymes. However, the C-terminal PDZ domain binding motif found in TRPC4 is absent in TRPC1. Thus, the molecular component(s) involved in the assembly of the TRPC1-associated protein complex is not yet known.

In recent years, much evidence has emerged which demonstrates that key molecules involved in Ca^{2+} signaling are associated with caveolar lipid rafts, thus implicating the importance of caveolae in Ca^{2+} signaling (13, 19–22). Lipid rafts are detergent-insoluble membrane domains formed by the dynamic clustering of sphingolipids and cholesterol which have been suggested to function as platforms for protein attachment, trafficking, and signaling (23–26). A specialized subset of lipid rafts, called caveolae, contains the cholesterol-binding protein caveolin, which provides a scaffold onto which molecules can concentrate to form signaling complexes at specific microdomains in the plasma membrane. This membrane specification facilitates coordination of incoming and outgoing cellular messages (26–29). Our finding that TRPC1 and TRPC3 form complexes with Ca^{2+} signaling proteins that are associated with caveolar domains strongly suggests that regulation of SOCE occurs within this complex. Consistent with our results, several recent studies show that TRPC1 (30, 31) and TRPC4 (32) are associated with caveolar lipid raft domains. In addition, integrity of the caveolar lipid domain is critical for SOCE and TRPC1 function (13, 31).

In this study we have examined the role of Cav1 in SOCE. Our data demonstrate that Cav1 regulates the plasma membrane localization of TRPC1 by binding to a site on its N terminus. Deletion of the Cav1 binding site in TRPC1 disrupts routing of TRPC1 to the

[1]The abbreviations used are: SOCE, store-operated Ca^{2+} entry; aa, amino acid(s); Ad, adenovirus; AEBSF, 4-(2-aminoethyl)-benzenesulfonyl fluoride; Cav, caveolin-1; CCh, carbachol; GFP, green fluorescent protein; GST, glutathione *S*-transferase; HA, hemagglutinin; HSG cells, human submandibular gland cells; MDCK, Madin-Darby canine kidney; Tg, thapsigargin; YFP, yellow fluorescent protein; TRPC, transient receptor potential canonical; INAD, inactivation-no-after potential D; OG, *n*-octyl-β-D-glycopyranoside.

plasma membrane and also suppresses SOCE. Together with our previous studies showing that TRPC1 is a component of SOCE channels (9, 33), the present data reveal a potentially important role for Cav1 in the plasma membrane assembly of SOCE channels.

EXPERIMENTAL PROCEDURES

Reagents

4-(2-Aminoethyl)-benzenesulfonyl fluoride (AEBSF), leupeptin, and pepstatin A were from Roche Applied Science, dithiothreitol was from Calbiochem, and aprotinin was from Sigma. Both the peroxidase-conjugated anti-HA antibody used for Western blotting and the high affinity rat anti-HA antibody used for immunofluorescence were from Roche Applied Science. The pEGFP-C3 vector and Living Colors (anti-YFP and anti-GFP) monoclonal antibody (JL-8) were from Clontech Laboratories (Palo Alto, CA). Cholera toxin subunit B, Alexa Fluor 594 conjugate was purchased from Molecular Probes (Eugene, Oregon). HA-conjugated affinity matrix beads was from Babco (Richmond, CA). Anti-FLAG antibody and affinity-agarose gel were from Sigma.

Plasmid Construction

The YFP-Cav1 plasmid was a generous gift from Dr. Junji Nishimura (Kyushu University, Fukoka, Japan). The YFP-Cav1Δ51–169 plasmid was constructed from the full-length YFP-Cav1 by PCR. Two oligonucleotides, 5′-GTCCACACCGTCTGTGACCCACTCTT and 5′-GTTGACCAGGTCGATCTCCTTGGTGTG, were used to amplify from the YFP-Cav1 to construct an N-terminal YFP-fusion, truncated fragment of Cav1 of about 5.1 kb using Takara Ex *Taq* DNA polymerase (Panvera, Madison, WI). The 3′-AT overhangs of the fragment were blunt ended using T4 DNA polymerase (New England Biolabs, Beverly, MA), and religated using a Rapid Ligation Kit (Roche Applied Science). The original YFP-Cav1 and religated YFP-Ca-v1Δ51–169 plasmids were subsequently used to transform *Escherichia coli*, individual clones were selected, and the insert was confirmed by sequencing from both directions prior to transfection of cells. The GFP-Cav1 plasmid was constructed by amplifying the hCav-1 gene using the following oligonucleotides: 5′-CTCGAGATGTCTGGGGGCAAATACGTAGACTCG and 5′-GGTACCAATATTTCTTTCTGCAAGTTGATGCGGAC. The PCR product was digested with *Xho*I and *Kpn*I and cloned in-frame into the pEGFP-C3 vector. The GFP-Cav1 plasmid was used to transform *E. coli*. Individual clones were selected and sequenced.

The two internal deletion TRPC1 plasmids, TRPC1Δ271–349 and TRPC1ΔCΔ271–349 (for details regarding TRPC1ΔC, see Ref. 15; the TRPC1 aa sequence is numbered to include the 8-aa HA sequence at the N terminus) were constructed as follows. The constructs were first amplified separately from two pairs of oligonucleotides: 1) 5′-ATCGATGTTTGGCCAGTCCAGCTCTAATAATG and 2) 5′-CTTCTTACAGGTGGGCTTGCGTCGCCGGGCTAGTTCCTCATAATCATT-CCTGAATTCC; as well as 3) 5′-CGACGCAAGCCCACCTGTAAGAAGATAATG and 4) 5′-GTATACATAAAAAAGAGACGAAGATAACTTAGAAC. The two PCR products, each containing a stretch of overlapping DNA sequence as shown in the above underlined nucleotides, were used as templates for another round of PCR reaction with primers 1 and 4. This last reaction produced a TRPC1 DNA fragment of 0.7 kb with an internal deletion from aa 271 to 349. It was restriction digested with *Hpa*I and *Esp*3I. The digested fragment was gel cleaned and cloned into either pcDNA3-HA-TRPC1 or pcDNA3-HA-Δtrp1 (15) to construct the two plasmids TRPC1Δ271–349 and TRPC1ΔCΔ271–349. The insert was confirmed by sequencing from both directions prior to transfection of cells. The internal deletion TRPC1 plasmid TRPC1Δ322–349 was constructed similarly by amplifying TRPC1 fragments using oligonucleotides 1 and 5

CTTCTTACAGGTGGGCTTGCGTCGGATAGCAAGTTTTAGACGACTTAAATTCATT CTTTC; and 3 and 4. The two PCR products were manipulated as described above to generate the desired TRPC1 deletion mutant.

Cell Culture and Transfection

Conditions for culturing and transfecting the human submandibular gland cells (HSG) have been described previously (9). Madin-Darby canine kidney (MDCK) cells were grown in Eagle's minimum essential medium, supplemented with 10% fetal calf serum, 2 mM L-glutamine, 100 units/ml penicillin, and 100 μg/ml streptomycin (all from Biofluids, Rockville, MD). To transfect cells stably with Cav1 plasmids, 1 μg of plasmid DNA was mixed with Lipofect-AMINE reagent 2000 (Invitrogen) in serum-free medium. Cells were incubated with this mixture for 5 h and then selected with 0.5 mg/ml G418 (Biofluids). Where indicated, control or HSG cells stably transfected with either YFP-Cav1 or YFP-ΔCav1 were infected with adenovirus encoding TRPC1 (Ad-TRPC1, 10), at 5 multiplicity of infection for either 24 or 48 h.

Protein Extraction and Western Blot Analysis

Cells were harvested from culture dishes, washed, and frozen as described previously (13). Frozen cells were thawed and homogenized with a Dounce homogenizer, diluted in sucrose buffer containing 0.25 M sucrose, 10 mM Tris-HEPES, pH 7.4, 1% (v/v) aprotinin, 1 mM dithiothreitol, 0.5 mM AEBSF, 0.167 mM pepstatin A, 0.167 mM leupeptin, and centrifuged at 1,600 × *g* for 15 min to remove the cell debris. The resulting supernatant was centrifuged at 30,000 × *g* for 1 h to obtain the lighter cytoplasmic fraction and the heavy membrane fraction. Both fractions were frozen and stored at −80 °C until further use. Where indicated, the cytoplasmic fraction was centrifuged further at 100,000 × *g* for 1 h to separate the soluble cytosolic fraction from the light membrane fraction. Protein concentration was determined using the Bio-Rad protein assay solution. Membranes were solubilized as described earlier (13). Proteins were separated on SDS-polyacrylamide gels and analyzed by Western blotting (13, 15). All primary antibodies were used at a dilution of 1:1,000 except for the horseradish peroxidase-conjugated HA and FLAG antibodies, which were used at 1:500.

Detergent Solubilization of HSG Cell Membranes and Immunoprecipitation

1 mg of membrane fraction was incubated on ice for 20 min with 1% Triton X-100 and 0.5 M KI in 500 μl of 50 mM Tris-HCl, pH 7, 150 mM NaCl, and 5 mM EDTA buffer. The sample was then centrifuged at 4 °C at 125,000 × *g* for 1 h, and the pellet was resuspended in 500 μl of the same buffer as above. Equal amounts of detergent-soluble and -insoluble proteins were loaded on SDS-polyacrylamide gels for Western analysis. Immunoprecipitation was carried out with OG + KI solubilized fraction of crude membranes. Antibodies (anti-YFP, anti-HA, and anti-FLAG) were used at 1:200 dilution. Anti-HA- or anti-FLAG-conjugated beads were used at a concentration of 50 μl/ml.

GST Fusion Protein Pull-down Assay

The N (aa 1–347) and C terminus (649–793) of TRPC1 were cloned into pGEX5.1 (Amersham Biosciences) vector using PCR-based strategy. Two liters each of *E. coli* (BL-21)-expressing GST-N-TRPC1 and GST-C-TRPC1 were induced with isopropyl-1-thio-β-D-galactopyranoside and purified as described (11). HSG cells expressing YFP-Cav1 or YFP-Cav1Δ51–169, either with or without HA-TRPC1, were harvested as described above. Frozen cells were thawed and homogenized with a Dounce homogenizer and sonicated (three times, 10 s each). An equal volume of 2× buffer containing 20 mM Tris-HEPES, pH 7.4, 300 mM NaCl, 2 mM dithiothreitol, 1 M KI, 3% OG was added to the cell

suspension. Samples were incubated on ice for 20 min and centrifuged at 145,000 × *g* for 1 h at 4 °C. 18 μg of purified GST-N-TRPC1 and 15 μg of GST-C-TRPC1 were incubated for 60 min with 1 mg of OG + KI-solubilized whole cell lysates. Proteins were pulled down with 80 μl of GST beads and washed three times with wash buffer. Proteins were released by boiling in SDS sample buffer, separated by SDS-PAGE, and identified by Western blotting.

Yeast Two-hybrid Assay

N-TRPC1 (aa 1–347), C-TRPC1 (aa 649–793), and five fragments of the TRPC1 N terminus (ΔN1, aa 1–86; ΔN2, aa 74–153; ΔN3, aa 143–213; ΔN4, aa 204–280; ΔN5, aa 271–349) were cloned into pGBKT7 (GAL4 DNA binding domain; Clontech). Cav1Δ80–169 (with deletion of aa 80–169 of Cav1) was cloned into pGADT7 (GAL4 DNA activation domain; Clontech). Plasmids were used to transform the yeast reporter strain AH 109 (Clontech), which was first grown on minimal synthetic dropout (SD) plates without leucine and tryptophan to select for transformants. Individual clones were further grown on SD plates without leucine, tryptophan, histidine, and adenine. Clones that grew on SD plates lacking all four amino acids were selected to be positive for protein-protein interaction. A β-galactosidase assay was performed to confirm and quantify the interactions as instructed by the Clontech Matchmaker System.

Immunofluorescence

HSG or MDCK cells were plated on coverslips for 1 day. They were then fixed and processed for confocal microscopy as described before (34). For lipid raft labeling, the cholera toxin conjugate was added to cells at a final concentration of 10 μg/ml and incubated for 20 min at 37 °C. Cells were washed three times with phosphate-buffered saline and fixed as described (34). Images were collected by confocal microscopy (9).

$[Ca^{+2}]_i$ Measurements

Fura2 fluorescence in single cells was measured by microfluorometry using a TILL Photonics spectrofluorometer (Polychrome 4, Applied Scientific Instrumentation and TILL Photonics Inc., Eugene, OR) attached to an inverted Nikon Diaphot microscope with a Fluor ×40 oil immersion objective. Images were acquired using an enhanced CCD camera (CCD-72, DAGE-MTI) and the MetaFluor software (Universal Imaging Corporation). Analog plots of the fluorescence ratio (340/380) are shown.

RESULTS

Interaction of TRPC1 with YFP-Cav1

YFP-Cav1 stably expressed in HSG cells displayed a punctate localization in the plasma membrane (*green* signal in *left panel*, Fig. 1*A*). In contrast, when YFP was expressed alone it was distributed uniformly over the entire cytoplasm (data not shown). Furthermore, the localization of YFP-Cav1 did not change if GFP was fused with the C terminus of Cav1 instead of YFP at the N terminus (data not shown). Localization of endogenous TRPC1 in HSG cells stably expressing YFP-Cav1 was examined using anti-TRPC1 antibody (33). Endogenous TRPC1 was localized in the plasma membrane and subplasma membrane regions (Fig. 1*A*, *middle panel*, *red* signal). Colocalization of YFP-Cav1 and endogenous TRPC1 was seen in the plasma membrane as a punctate yellow signal (Fig. 1*A*, *right panel*, *yellow* signal). Consistent with our results, endogenous TRPC1 has been shown previously to colocalize with Cav1 in the plasma membrane of mouse sperms (30). Control samples showed that there was no contribution of the YFP fluorescence to the red signal (image not shown). Fig. 1*B* shows the immunolocalization of exogenously expressed HA-TRPC1 in HSG cells stably expressing YFP-Cav1 (Ad-TRPC1 was used to express HA-TRPC1 in

YFP-Cav1 cells transiently). Consistent with the localization of YFP-Cav1 (Fig. 1*B*, *upper left panel*, *green* signal), HA-TRPC1 was also primarily detected in the plasma membrane and perinuclear region (Fig. 1*B*, *upper right panel*, *red* signal). Overlay of the HA and YFP signals demonstrated a distinct punctate plasma membrane colocalization of the two proteins (Fig. 1*B*, *lower left panel*, *yellow* signal). This was confirmed further by overlaying this image on a differential interference contrast image (Fig. 1*B*, *lower right panel*). The colocalization of TRPC1 and Cav1 was also demonstrated in another epithelial cell line, MDCK. As seen in HSG cells, stably expressed YFP-Cav1 and transiently expressed HA-TRPC1 were colocalized in the plasma membrane region (Fig. 1*C*). Thus, plasma membrane colocalization of TRPC1 and Cav1 was not restricted to HSG cells.

Colocalization of Cav1 and TRPC1 proteins was confirmed further by immunoprecipitation of YFP-Cav1 with HA-TRPC1 (Fig. 1*D*). Both proteins were detected in the OG + KI-solubilized fraction of crude membranes isolated from cells expressing YFP-Cav1 and HA-TRPC1 (Fig. 1*D*, *lane 1*). The proteins were also detected in the immunoprecipitate (immunoprecipitates with anti-YFP antibody; Western blots using either anti-HA or anti-YFP antibodies (Fig. 1*D*, *lane 2*; note that these bands are not seen in control immunoprecipitates from nontransfected cells, data not shown). Together with our previous reports showing that endogenous TRPC1 or exogenously expressed TRPC1 is immunoprecipitated with endogenous Cav1 in HSG cells (13, 15), these data suggest that TRPC1 and Cav1 interact with each other. To examine this interaction in greater detail, GST fusion proteins of the N or C terminus of TRPC1 were made. Lysates from HSG cells expressing YFP-Cav1 (Fig. 1*E*, *second lane*) were passed through columns containing GST-N-TRPC1 or GST-C-TRPC1. YFP-Cav1 interacted with both the N and C terminus of TRPC1, although there was more binding with the C terminus (Fig. 1*E*, *third* and *fourth lanes*). Fig. 1*E*, *first lane*, shows that control GST protein does not bind Cav-1.

Identification and Functional Characterization of the Cav1 Binding Domain in the N Terminus of TRPC1

The data in Fig. 1 are consistent with our previous suggestion that TRPC1 has putative caveolin binding domains in both the N and C terminus (13). Although further studies will be required to determine the functional consequences of the binding of the C terminus of TRPC1 to Cav1, we have reported previously that C-terminal deletion of TRPC1 does not affect its plasma membrane localization or decrease SOCE (11, 15). Therefore, we investigated further the Cav1 binding site on the TRPC1 N terminus. A mutant of Cav1 was constructed, Cav1Δ80–169, which lacked the scaffolding domain, membrane anchoring domain, and the three palmitoylation sites and thus could be used in a yeast two-hybrid assay. Interactions between this Cav1 mutant and the N and C terminus of TRPC1 were examined. Cav1Δ80–169 interacted with the TRPC1 N terminus but not the C terminus (Fig. 2*A*) thus providing us with a useful tool to examine Cav1 interactions with the TRPC1 N terminus.

To map the Cav1 binding domain in the TRPC1 N terminus, sequences of TRPC1, shown in Fig. 2*B*, were cloned into the yeast two-hybrid vectors and screened against Cav1Δ80–169. Significant interaction was seen between Cav1 and ΔN5, aa 271–349 (Fig. 2*C*). To determine the role of this Cav1 binding domain in TRPC1 function, aa 271–349 were deleted in HA-TRPC1 (HA-TRPC1Δ271–349, Fig. 3*A*), and the protein was expressed in MDCK (Fig. 3*B*, *left panel*) or HSG cells (Fig. 3*B*, *middle panel*). In either cell type, plasma membrane localization of the protein was disrupted, and an intracellular localization was seen. Similar deletion was made in the N terminus of TRPC1Δ664–793, which lacks the entire C terminus (HA-TRPC1ΔCΔ271–349; Fig. 3*A*), and the protein was expressed in HSG. Although TRPC1Δ664–793 was localized in the plasma membrane region (not shown here, see Ref. 15), further deletion of aa 271–349 in this protein disrupted its plasma

membrane localization (Fig. 3*B*, *right panel*). Fig. 3*C* shows the expression of HA-TRPC1Δ271–349 and HA-TRPC1ΔCΔ271–349 compared with that of full-length HA-TRPC1.

Further, SOCE was measured in cells transiently expressing HA-TRPC1Δ271–349 (Fig. 3*D*). Thapsigargin (Tg)-stimulated internal Ca^{2+} release was not altered significantly by the expression of HA-TRPC1Δ271–349 in HSG cells. When 1 m_M calcium was added externally, control HSG cells showed an immediate increase in internal [Ca^{2+}] (Fig. 3*D*, *left panel*). Importantly, this increase, representing SOCE, was significantly decreased in HSG cells expressing TRPC1Δ271–349 compared with that in control HSG cells (Fig. 3*D*, *right panel*; for average data, see also Fig. 3*E*). Thus, in contrast to expression of full-length HA-TRPC1, which induces an increase in SOCE, HA-TRPC1Δ271–349 induced a dominant suppression of SOCE.

We had suggested previously that the TRPC1 sequence aa 322–349 includes the caveolin binding motif (13). Importantly, this motif appears to be conserved in a number of TRPC proteins (Fig. 4*A*). Thus, we deleted aa 322–349 in TRPC1 (HA-TRPC1Δ322–349, Fig. 4*B*) and expressed this protein in HSG cells. Consistent with the results shown in Fig. 3*C*, deletion of this domain from TRPC1 altered the localization of the protein. TRPC1 was seen to be distributed intracellularly rather than in the plasma membrane (Fig. 4*C*, compare *left panel w*ith *middle* and *right panels*). Further, SOCE was also suppressed in these cells (data not shown). TRPC1 monomers have been suggested to form homomultimers via N-terminal interactions (33, 35, 36). Based on these previous studies, we suggest that HA-TRPC1Δ271–349 and HA-TRPC1Δ322–349 likely interact with endogenous TRPC1 and retain it intracellularly. This would induce a decrease in functional plasma membrane SOCE channels and account for the decrease in SOCE. This is demonstrated in Fig. 4*D*, which shows that HA-TRPC1Δ322–349 was immunoprecipitated with FLAG-TRPC1 when the two proteins were coexpressed, demonstrating that it retains the ability to interact with wild-type TRPC1. These data can account for the suppression of SOCE in cells expressing the mutant TRPC1 proteins. In aggregate, the results presented above strongly suggest that the N-terminal Cav1 binding domain, aa 322–349, of TRPC1 is involved in the plasma membrane localization of the protein and thus contributes to SOCE.

Effect of YFP-Cav1Δ51–169 on SOCE

To understand further the role of Cav1 in TRPC1 localization, we examined the effect of a Cav1 mutant that lacked the protein scaffolding and membrane anchoring domains (with YFP fused at the N terminus, YFP-Cav1Δ51–169). Fig. 5*A* shows that YFP-Cav1Δ51– 169 is pulled down by GST-N-TRPC1 but not GST-C-TRPC1. Because YFP-Cav1Δ51–169 lacks its proposed protein scaffolding domain, we presently do not understand how it binds to GST-N-TRPC1. It is likely that other domains of Cav-1 or oligomerization with WT-Cav1 are involved in this interaction. When stably expressed in HSG cells, YFP-Cav1Δ51–169 displayed an intracellular localization that was diffused over the entire cytoplasm and the nucleus (Fig. 5, *B* and *C*, *left panels, green* signal). Importantly, in cells expressing YFP-Cav1Δ51–169, there was a diffused intracellular localization of endogenous TRPC1 (Fig. 5*B*, *middle panel*, *red* signal), or exogenously expressed HA-TRPC1 (Fig. 5*C*, *middle panel*, *red* signal). Furthermore, there was no colocalization of TRPC1 and YFP-Cav1Δ51–169 in the plasma membrane region of these cells, but rather overlay of red and green fluorescence was detected inside the cells (see *arrowheads* in Fig. 5, *B* and *C*, *right panels*, *yellow* signal; compare with localization of *yellow* signal in Fig. 1).

The effect of YFP-Cav1Δ51–169 on Carbachol (CCh)- and Tg-stimulated Ca^{2+} increases was also measured (Fig. 5, *D*–*G*). In YFP-Cav1Δ51–169-expressing HSG cells, the SOCE was substantially delayed and significantly lower (compare second peaks in Fig. 5, *D* and *F*,

with those in Fig. *E* and *G*). Fig. 5, *H* and *I*, show average data and statistical evaluations. In separate experiments, HA-TRPC1 was transiently expressed in YFP-Cav1Δ51–169-expressing cells or in control HSG cells, and similar procedures were carried out (traces not shown). Tg- or CCh-stimulated SOCE was significantly higher in HSG cells infected with Ad-TRPC1 (average peak fluorescence ratios were 5.7 ± 0.22 and 6.04 ± 0.32 in TRPC1-expressing cells compared with 3.5 ± 0.42 and 4.2 ± 0.35 in control cells with CCh and Tg, respectively). However, when TRPC1 was coexpressed in YFP-Cav1Δ51–169-expressing cells, SOCE was significantly lower compared with the control HSG cells (average data as shown in Fig. 5, *J* and *K*).

Membrane Interactions and Detergent Solubility of YFP-Cav1Δ51–169 and TRPC1

Fig. 6*A* shows subcellular fractions from control HSG cells (*1*), and cells expressing the full-length (*2*) or mutant (*3*) YFP-Cav-1. YFP-Cav1 was relatively enriched in the light and heavy membrane fraction (*Lm* and *Hm*, respectively). On the other hand, most of the YFP-Cav1Δ51–170 proteins remained in the cytosolic fraction (*Cs*). We also examined the presence of HA-TRPC1 in these same cellular fractions using anti-HA antibody (Fig. 6*B*). The expressed HA-TRPC1 was relatively enriched in the heavy membrane fraction in control HSG cells as well as cells stably expressing the YFP-Cav1 or YFP-Cav1Δ51–170. However, more TRPC1 associated with the lighter membrane fraction in Cav1Δ51–170 cells than in Cav1 cells (compare *Lm* in *2* and *3*).

Detergent (Triton X-100) insolubility of proteins has been used as a criterion for their association with lipid rafts (23, 29). Previously we showed that a major proportion of the endogenous TRPC1 in HSG cells is detergent-insoluble (13). Here we examined the detergent solubility of the full-length and mutant caveolins as well as that of HA-TRPC1 in HSG cell expressing these exogenous caveolins. YFP-Cav1 was relatively enriched in the Triton X-100-resistant pellet (Fig. 6*C*, *2-P*). In contrast, the small fraction of YFP-Cav1Δ51–170 which was associated with membranes was completely solubilized by Triton X-100 (Fig. 6*C*, *3-S*). In the control HSG cells, HA-TRPC1 was relatively enriched in the Triton X-100-insoluble pellet, although it was also detected in the soluble fraction (Fig. 6*D*, *first* and *second lanes*). HA-TRPC1 in cells expressing YFP-Cav1 was much more enriched in the Triton X-100-resistant pellet than in the soluble fraction (Fig. 6*D*, *third* and *fourth lanes*). Importantly, HA-TRPC1 in cells expressing YFP-Cav1Δ50–170 was relatively more soluble in Triton X-100 (Fig. 6*D*, *fifth* and *sixth lanes*). Together with the immunolocalization pattern of TRPC1, these data suggest that the localization of HA-TRPC1 in caveolar-lipid raft domains is disrupted by expression of YFP-Cav1Δ50–170. However, this was not caused by a general disruption of plasma membrane lipid raft domains, as assessed by examining the binding of cholera toxin subunit B conjugate to HSG cells (37). Full-length Cav1 is localized to the plasma membrane, whereas the truncated Cav1 is detected in intracellular region in HSG cells (Fig. 6*E*). Cholera toxin similarly labeled the plasma membrane in control HSG cells and in cells expressing either the full-length or truncated Cav1 (Fig. 6*F*). Some signal was also detected inside the cell, suggesting internalization of a small amount of toxin during the incubation period.

DISCUSSION

A large number of studies have demonstrated that SOCE occurs within a spatially restricted plasma membrane domain in cells. It has been proposed that the architecture of this domain facilitates a direct physical, or a functional, coupling between the molecular components which leads to activation, or inactivation, of plasma membrane SOCE channels (2, 13, 17, 38). Recently, evidence has been provided for the localization of a number Ca^{2+} signaling proteins within caveolar lipid raft domains in the plasma membrane (19, 22). Furthermore, SOCE has been reported to require intact lipid rafts (13, 19). We have reported previously

that TRPC1 and TRPC3 are associated with the scaffolding protein, Cav1, and are assembled in a protein complex with key Ca^{2+} signaling proteins (13–15). Additionally, we have shown that TRPC1 is a critical component of SOCE channels in HSG cells (9, 33). Thus, we suggested earlier that regulation of the SOCE channel is achieved by protein-protein interactions within the TRPC1-associated signaling complex and/or by recruitment of additional proteins into the complex (13). However, the exact mechanisms involved in the regulation of SOCE are not known, and the role of Cav1 in this process is also not yet elucidated. The *Drosophila* TRP is assembled in a signaling complex (3, 4). Components of this signalplex are assembled in the rhabdomere via interaction with the scaffolding protein INAD, which contains several PDZ domains and also forms oligomers (12). Mutations in INAD or in the INAD-interacting domain of TRP result in disruption of the signalplex and loss of function. Recently, INAD was shown to act as a suppressor of TRPC function when expressed in Sf9 cells (39). Thus, information regarding the assembly of the mammalian TRPC1-associated signaling complex is key to understanding the mechanism involved in SOCE.

The data presented above demonstrate that Cav1 is a critical protein in the mechanism of SOCE. Consistent with our previous suggestions (13), the present data demonstrate that there are two caveolin binding sites in TRPC1. Significantly, deletion of the N-terminal Cav1 binding domain in full-length or C-terminal truncated TRPC1 prevented plasma membrane localization of the protein. In contrast, we have reported earlier that truncation of the C terminus itself, which includes the C-terminal Cav1 binding site, does not alter localization of TRPC1 (11, 15). These data suggest that plasma membrane localization of TRPC1 depends on the interaction of its N terminus, but not the C terminus, with Cav1. We have further shown that plasma membrane localization of both endogenous and exogenously expressed TRPC1 was disrupted when a mutant Cav1, lacking its protein scaffolding and membrane anchoring domains, was expressed in the cells. Our data show that this was not because of a generalized disruption of plasma membrane lipid raft domains. We have also shown that this mutant Cav1 interacts with wild-type TRPC1, although we do not yet understand how it interacts with TRPC1. However, because it lacks the membrane scaffolding domains, we hypothesize that the effect on TRPC1 localization is caused by the inability of this mutant Cav1 to anchor to the plasma membrane.

The role of Cav1 in the plasma membrane localization of TRPC1 is more clearly shown by our data that TRPC1 lacking the N-terminal Cav1 binding domain is not localized in the plasma membrane and failed to increase SOCE. Instead, it exerted a dominant negative effect on the SOCE and significantly reduced Tg-stimulated Ca^{2+} influx. In contrast, full-length TRPC1 induced a 1.5–2.0-fold increase in SOCE. Together with our data showing that this mutant TRPC1 can interact with wild-type TRPC1, these data strongly suggest that TRPC1-Cav1 interactions play an important role in the generation of functional SOCE channels in the plasma membrane. Previously reported studies suggest that TRPC1 monomers interact with each other and with other TRPC proteins to form SOCE channels (35, 36, 40). Consistent with this, we have also observed that exogenously expressed TRPC1 interacts with each other and with the endogenous TRPC1 protein in HSG cells (33). Based on these data we suggest that TRPC1 lacking the N-terminal Cav1 domain interacts with the endogenous TRPC1 protein in HSG cells and thus prevents it from being routed to the plasma membrane. The resulting decrease in functional SOCE channels on the cell surface accounts for the loss of SOCE. An important implication of these data is that coassembly of the TRPC monomers takes place prior to plasma membrane insertion. An alternative explanation of our data is that TRPC1-Cav1 interaction is required for the retention of TRPC1 heteromers in the plasma membrane. Further studies will be needed to determine whether Cav1 is the scaffold that allows retention of TRPC1 in the plasma membrane or if it is involved in trafficking of the protein to the cell surface where it is assembled into SOCE

channels. Irrespective of this, our data demonstrate that Cav1 has an important role in plasma membrane organization of functional TRPC1-containing SOCE channels.

Our data also suggest that not all components in the TRPC1 signaling complex are trafficked together. We have shown that CCh-stimulated internal Ca^{2+} release is not altered by expression of Cav1Δ51–169, which demonstrates that the signaling proteins proximal to TRPC1 are functionally intact. A number of signaling proteins that are acylated, such as H-ras and G_a subunit of heterotrimeric G proteins, do not require Cav1 for sorting to the plasma membrane caveolae. Rather, they are trafficked directly to the plasma membrane and are anchored to the caveolae via their acyl side chains. TRPC1, however, does not appear to have any known consensus sequences for lipid modification. This is consistent with our suggestion that TRPC1 is recruited to the plasma membrane via a direct interaction of its N terminus with Cav1. Our data demonstrate that Cav1 is required for the localization of TRPC1 in plasma membrane lipid raft domains. Further, we have shown that the biochemical characteristics of TRPC1 are altered in cells expressing Cav1Δ51–169. TRPC1 from these cells was relatively more soluble in detergent than from cells expressing full-length Cav1. Consistent with this, the biochemical characteristics of YFP-Cav1Δ51–169 were dramatically altered compared with those of full-length caveolin. It was relatively enriched in the cytosolic fraction rather than in the membrane fraction, and the small fraction of this protein that was membrane-associated appeared to be completely soluble in Triton X-100. In aggregate, these data demonstrate that interaction of TRPC1 with Cav1 plays a critical role in the trafficking of TRPC1 to plasma membrane lipid raft domains where it is assembled into a signaling complex with other key Ca^{2+} signaling proteins. Our present study does not exclude the possibility that Cav1 might exert additional effects on TRPC1 via its binding to the C terminus. For example, apart from acting as a platform for the assembly of signaling complexes, Cav1 also functions as a negative regulator holding signaling proteins such as eNOS, protein kinase C, and heterotrimeric G protein, in a basal, resting state (41, 42) and is involved in vesicular trafficking (43).

In conclusion, although SOCE was first described more than a decade ago, the mechanisms involved in its regulation are not yet known. An increasing number of studies suggest that SOCE is associated with a plasma membrane signaling complex that includes key Ca^{2+} signaling proteins. Consistent with this, a number of TRPC channels, *e.g.* TRPC1, TRPC3, and TRPC4, have been reported to be associated with one or more members of this signalplex. Previous studies from our laboratory and others have shown that TRPC1 is a molecular component of SOCE channels in several cell types (5–8, 9–11, 15, 33). Further, we had reported that TRPC1 is assembled in a signaling complex with Cav1 (13–15). Here we have demonstrated that plasma membrane localization of TRPC1 depends on an N-terminal Cav1 binding site. Importantly, disruption of plasma membrane localization of TRPC1 suppressed SOCE. Based on our present and previous data, we suggest that Cav1 contributes to the assembly of TRPC1-containing SOCE channels in plasma membrane caveolar lipid raft domains. Further studies will be required to determine exactly how stimulation of the Ca^{2+} signaling cascade results in activation of these SOCE channels.

Acknowledgments

We thank Dr. Junji Nishimura, Kyushu University, Fukuoka, for the YFP-Cav1 plasmid and Dr. Craig Montell for the FLAG-TRPC1 plasmid. We also thank Dr. Klaus Groschner for help.

REFERENCES

1. Putney JW Jr, Broad LM, Braun FJ, Lievremont JP, Bird GS. J. Cell Sci. 2001; 114:2223–2229. [PubMed: 11493662]
2. Minke B, Cook B. Physiol. Rev. 2002; 82:429–472. [PubMed: 11917094]

3. Zitt C, Halaszovich CR, Luckhoff A. Prog. Neurobiol. 2002; 66:243–264. [PubMed: 11960680]
4. Montell C. Science's STKE. 2001 http://www.stke.org/cgi/content/full/OC_sigtrans;2000/90/re1.
5. Antoniotti S, Lovisolo D, Fiorio Pla A, Munaron L. FEBS Lett. 2002; 510:189–195. [PubMed: 11801252]
6. Brough GH, Wu S, Cioffi D, Moore TM, Li M, Dean N, Stevens T. FASEB J. 2001; 15:1727–1738. [PubMed: 11481220]
7. Xu SZ, Beech DJ. Circ. Res. 2001; 88:84–87. [PubMed: 11139478]
8. Mori Y, Wakamori M, Miyakawa T, Hermosura M, Hara Y, Nishida M, Hirose K, Mizushima A, Kurosaki M, Mori E, Gotoh K, Okada T, Fleig A, Penner R, Iino M, Kurosaki T. J. Exp. Med. 2002; 195:673–681. [PubMed: 11901194]
9. Liu X, Wang W, Singh BB, Lockwich T, Jadlowiec J, O'Connell B, Weller R, Zhu MX, Ambudkar IS. J. Biol. Chem. 2000; 275:3403–3411. [PubMed: 10652333]
10. Singh BB, Zheng C, Liu X, Lockwich T, Liao D, Zhu MX, Birnbaumer L, Ambudkar IS. FASEB J. 2001; 15:1652–1654. [PubMed: 11427516]
11. Singh BB, Liu X, Tang J, Zhu MX, Ambudkar IS. Mol. Cell. 2002; 9:739–750. [PubMed: 11983166]
12. Li HS, Montell C. J. Cell Biol. 2000; 150:1411–1422. [PubMed: 10995445]
13. Lockwich TP, Liu X, Singh BB, Jadlowiec J, Weiland S, Ambudkar IS. J. Biol. Chem. 2000; 275:11934–11942. [PubMed: 10766822]
14. Lockwich T, Singh BB, Liu X, Ambudkar IS. J. Biol. Chem. 2001; 276:42401–42408. [PubMed: 11524429]
15. Singh BB, Liu X, Ambudkar IS. J. Biol. Chem. 2000; 275:36483–36486. [PubMed: 10980191]
16. Suh P-G, Hwang J-I, Ryu SH, Donowitz M, Kim JH. Biochem. Biophys. Res. Commun. 2001; 288:1–7. [PubMed: 11594744]
17. Venkatachalam K, van Rossaum DB, Patterson RL, Ma H-T, Gill D. Nat. Cell Biol. 2002; 11:E263–E272. [PubMed: 12415286]
18. Tang Y, Tang J, Chen Z, Trost C, Flockerzi V, Li M, Ramesh V, Zhu MX. J. Biol. Chem. 2000; 275:37559–37564. [PubMed: 10980202]
19. Isshiki M, Anderson RG. Cell Calcium. 1999; 26:201–208. [PubMed: 10643558]
20. Parton RG. Science. 2001; 293:2404–2405. [PubMed: 11577223]
21. Isshiki M, Ying YS, Fujita T, Anderson RGW. J. Biol. Chem. 2002; 277:43389–43398. [PubMed: 12177060]
22. Liu P, Michael R, Anderson RGW. J. Biol. Chem. 2002; 277:41295–41298. [PubMed: 12189159]
23. Brown DA, Rose JK. Cell. 1992; 68:533–544. [PubMed: 1531449]
24. Simons K, Ikonen E. Nature. 1997; 387:569–572. [PubMed: 9177342]
25. Hooper NM. Mol. Membr. Biol. 1999; 16:145–156. [PubMed: 10417979]
26. Simons K, Toomre D. Nat. Rev. Mol. Cell. Biol. 2000; 1:31–39. [PubMed: 11413487]
27. Rothberg KG, Heuser JE, Donzell WC, Ying Y, Glenney JR, Anderson RG. Cell. 1992; 68:673–682. [PubMed: 1739974]
28. Anderson RG. Proc. Natl. Acad. Sci. U. S. A. 1993; 90:10909–10913. [PubMed: 8248193]
29. Sargiacomo M, Sudol M, Tang Z, Lisanti MP. J. Cell Biol. 1993; 122:789–807. [PubMed: 8349730]
30. Trevino CL, Serrano CJ, Beltran C, Felix R, Darszon A. FEBS Lett. 2001; 509:119–125. [PubMed: 11734218]
31. Kunzelmann-Marche C, Freyssinet J, Martinez MC. J. Biol. Chem. 2002; 277:19876–19881. [PubMed: 11909856]
32. Torihashi S, Fujimoto T, Trost C, Nakayama S. J. Biol. Chem. 2002; 277:19191–19197. [PubMed: 11897792]
33. Liu X, Singh BB, Ambudkar IS. J. Biol. Chem. 2003; 278:11337–11343. [PubMed: 12536150]
34. Wang W, O'Connell B, Dykeman R, Sakai T, Delporte C, Swaim W, Zhu MX, Birnbaumer L, Ambudkar IS. Am. J. Physiol. 1999; 276:C969–C979. [PubMed: 10199829]

35. Xu X-Z, Chien F, Butler A, Salkoff L, Montell C. Neuron. 2000; 26:647–657. [PubMed: 10896160]
36. Engelke M, Friedrich O, Budde P, Schafer C, Niemann U, Zitt C, Jungling E, Rocks O, Luckhoff A, Frey J. FEBS Lett. 2002; 523:193–199. [PubMed: 12123831]
37. Janes PW, Ley SC, Magee AI. J. Cell Biol. 1999; 147:447–461. [PubMed: 10525547]
38. Kiselyov K, Mignery GA, Zhu MX, Muallem S. Mol. Cell. 1999; 4:423–429. [PubMed: 10518223]
39. Harteneck C, Kuchta SN, Huber A, Paulsen R, Schultz G. FASEB J. 2002; 16:1668–1670. [PubMed: 12206995]
40. Lintschinger B, Balzer-Geldsetzer M, Baskaran T, Graier WF, Romanin C, Zhu MX, Groschner K. J. Biol. Chem. 2000; 275:27799–27805. [PubMed: 10882720]
41. Razani B, Schlegel A, Lisanti MP. J. Cell Sci. 2000; 113:2103–2109. [PubMed: 10825283]
42. Galbiati F, Razani B, Lisanti MP. Cell. 2001; 106:403–411. [PubMed: 11525727]
43. Karlsson M, Thorn H, Parpal S, Stralfors P, Gustavsson J. FASEB J. 2002; 16:249–251. [PubMed: 11744627]

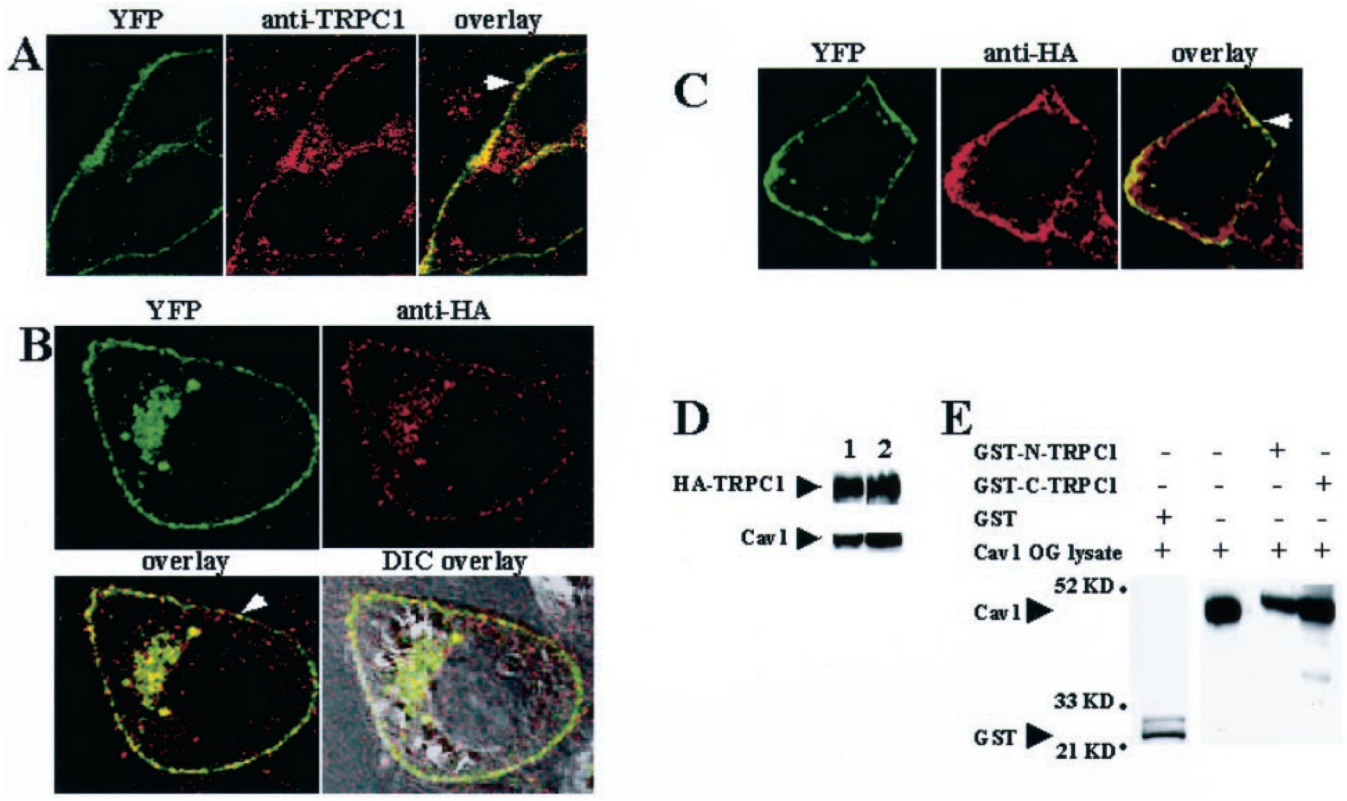

Fig. 1. Colocalization of TRPC1 and caveolin-1

A–C, confocal images showing localization of YFP-Cav1 (*A–C*), endogenous TRPC1 (*A*), and exogenously expressed HA-TRPC1 (*B* and *C*) in HSG cells (*A* and *B*) and MDCK cells (*C*). Cells stably expressing YFP-Cav1 were infected with Ad-TRPC1 to express HA-TRPC1 transiently. Proteins were detected using the YFP signal (*A–C*) and by anti-TRPC1 antibody (*A*), or anti-HA antibody, and rhodamine-linked secondary antibody (*B* and *C*). Cells were visualized using a ×100 objective. Other details are given under "Experimental Procedures." *D*, immunoprecipitation of YFP-Cav1 and HA-TRPC1. Detection of HA-TRPC1 and YFP-Cav1 in solubilized membrane fractions of HSG cells expressing YFP-Cav1 protein and HA-TRPC1 (*lane 1*) and in immunoprecipitates (*lane 2*) using anti-YFP antibody (blotting with anti-HA or anti-YFP) is shown. *E*, interaction of YFP-Cav1 with TRPC1. Cell lysates of HSG cells stably transfected with YFP-Cav1 and infected with Ad-TRPC1 (*second lane*) were poured over either GST-N-TRPC1 (*third lane*) or GST-C-TRPC1 (*fourth lane*). The fractions bound to the beads were analyzed by Western blotting using anti-YFP antibody. The experiment was repeated using lysates from cells without HA-TRPC1 expression, and the results were essentially the same (data not shown). Control GST-protein did not pull down Cav1 (*first lane*).

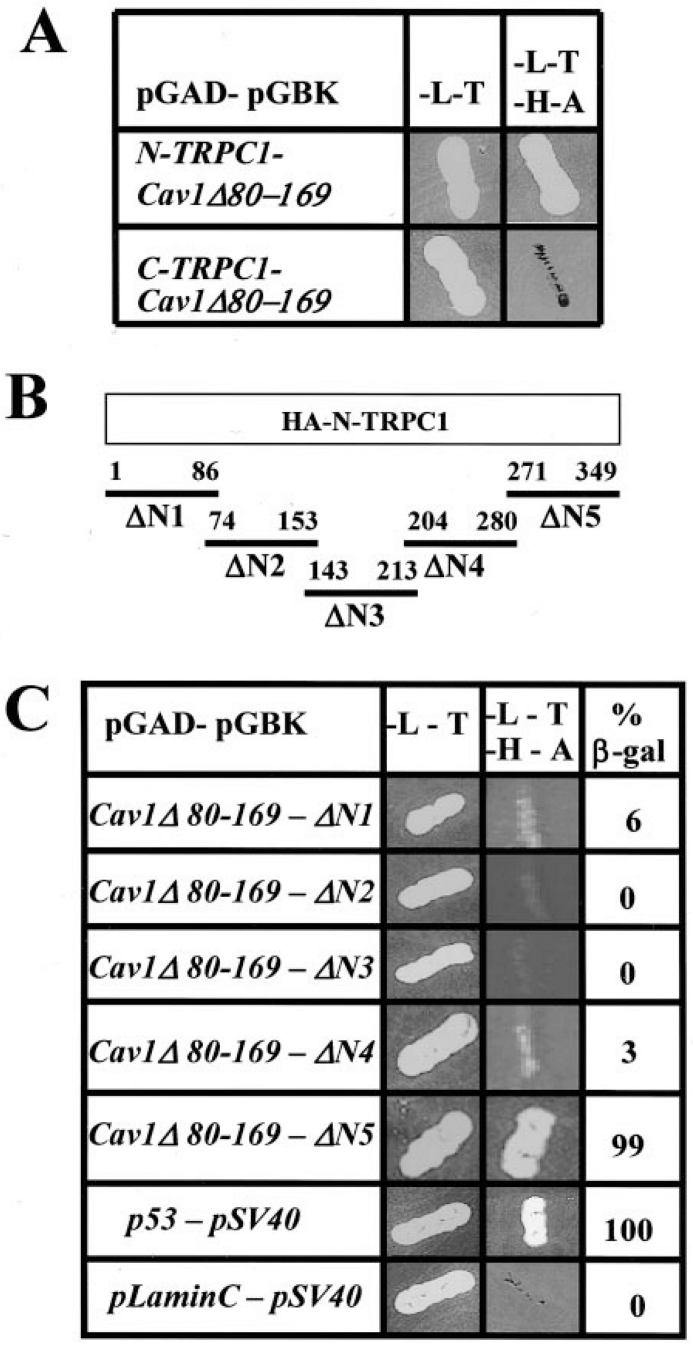

Fig. 2. Mapping the caveolin-binding domain in TRPC1

A, yeast two-hybrid analysis of interaction between TRPC1 and Cav-1 (for details, see "Experimental Procedures"). *B*, N-terminal regions of TRPC1 tested for interaction with Cav-1. *C*, yeast two-hybrid analysis of interaction of N-terminal fragments of TRPC1 with Cav-1. 34 units of β-galactosidase (β-*gal*) activity were detected with ΔN5 (β-gal activity was 35 units in the positive control) and were considered positive. β-Galactosidase activity <10% of that in the positive control was considered negative.

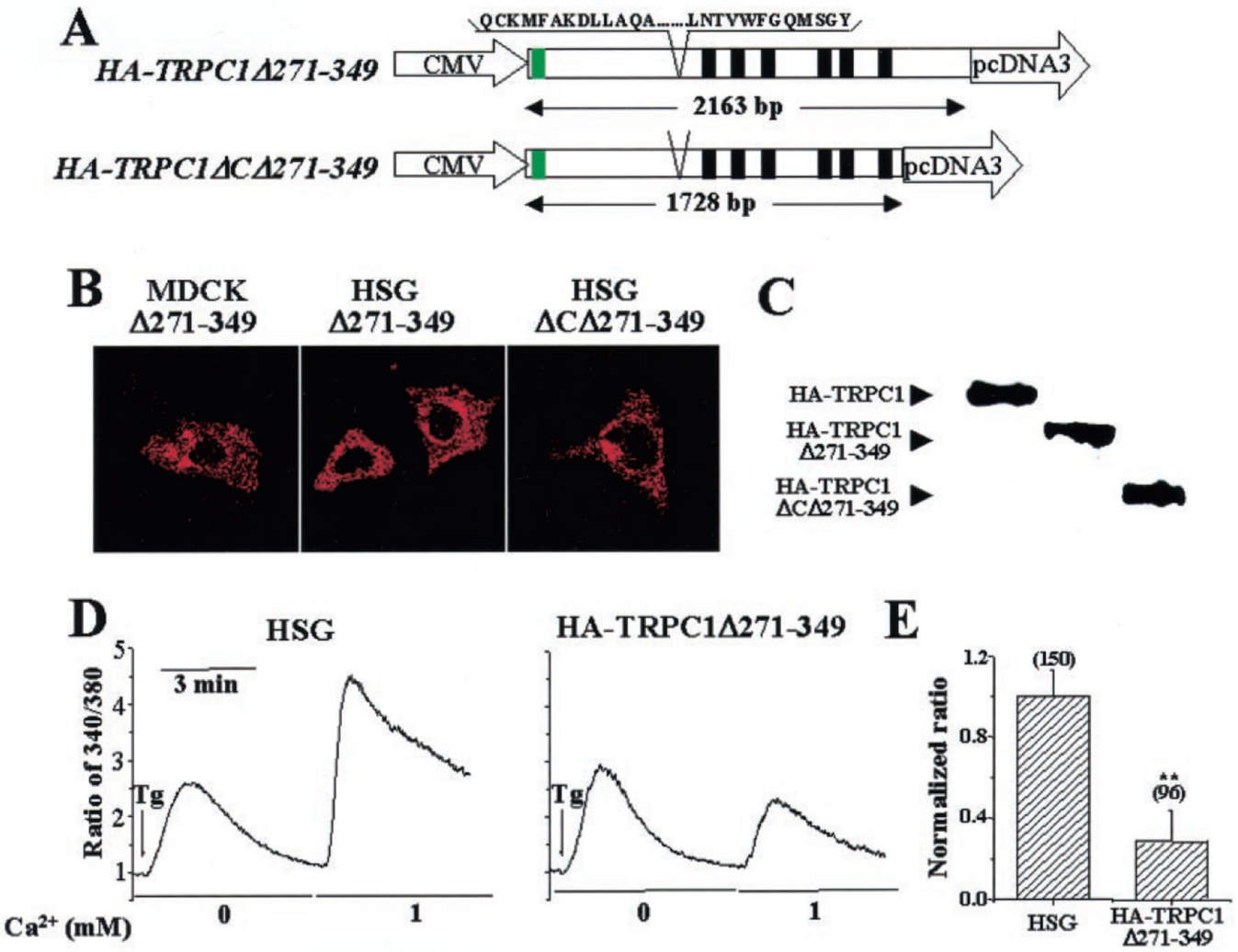

Fig. 3. Functional characterization of the TRPC1 N-terminal Cav1 binding domain

A, deletion of aa 271–349 in full-length and C-terminal truncated HA-TRPC1. *Green box*, HA tag at the TRPC1 N terminus. *Black boxes*, transmembrane domains. *CMV*, cytomegalovirus. *B*, localization of HA-TRPC1Δ271–349 in MDCK and HSG cells (*left* and *middle panels*, respectively) and HA-TRPC1ΔC lacking aa 271–349 (*right panel*). Images were acquired by confocal microscopy (×63 objective) using anti-HA antibody and rhodamine-labeled secondary antibody. *C*, Western blots showing expression of HA-tagged TRPC1, TRPC1Δ271–349, and TRPC1ΔCΔ271–349. Protein was detected using anti-HA antibody. *D*, fluorescence traces of Tg-stimulated Ca^{2+} influx in control HSG cells and cells expressing HA-TRPC1Δ271–349. Cells were stimulated in calcium-free buffer, and then 1 mM Ca^{2+} was added to the medium. *E*, *bar graphs* showing the average values expressed relative to that in control cells. *Asterisks* indicate values significantly different from control cells ($p < 0.02$).

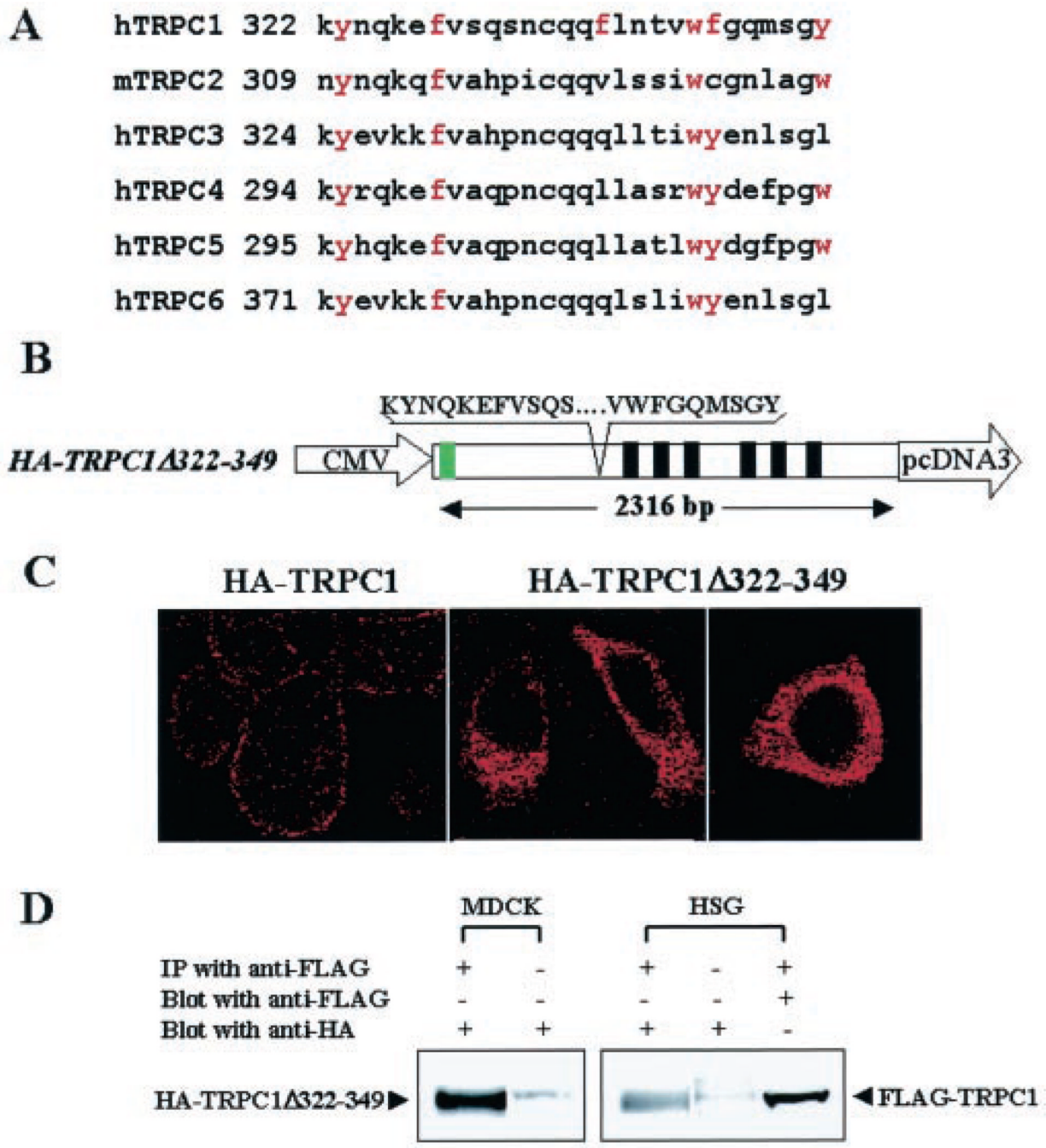

Fig. 4. Effect on TRPC1 localization by deletion of Cav1 binding domain

A, alignment of the putative Cav-1 binding domain in the N terminus of TRPC proteins. *B*, deletion of aa 322–349 in full-length TRPC1. *Green box*, HA tag at the TRPC1 N terminus. *Black boxes*, transmembrane domains. *CMV*, cytomegalovirus. *C*, localization of control HA-TRPC1 (*left panel*) and HA-TRPC1Δ322–349 (*middle* and *right panels*, respectively) in HSG cells. Images were acquired by confocal microscopy with either ×63 (*left* and *middle panels*) or ×100 (*right panel*) using anti-HA antibody and rhodamine-labeled secondary antibody. *D*, coimmunoprecipitation of TRPC1Δ322–349 with FLAGTRPC1. HSG or MDCK cells stably expressing FLAG-TRPC1 were transiently transfected with plasmid encoding TRPC1Δ322–349. Cells were lysed, and crude membranes were prepared and

solubilized as described under “Experimental Procedures.” Anti-FLAG antibody was used for immunoprecipitation (*IP*), and HA-TRPC1Δ322–349 was detected using anti-HA antibody on Western blots. *First lane*, immunoprecipitate from MDCK cells; *second lane*, OG extract from MDCK cells; *third lane*, immunoprecipitate from HSG cells; *fourth lane*, OG extract from HSG cells; *fifth lane*, blot in *third lane* was stripped and blotted with anti-FLAG antibody. OG extracts from 3 mg of crude membranes were used for immunoprecipitation (*first*, *third*, and *fifth lanes*). 30 μg of OG extract was loaded in the *second* and *fourth lanes*.

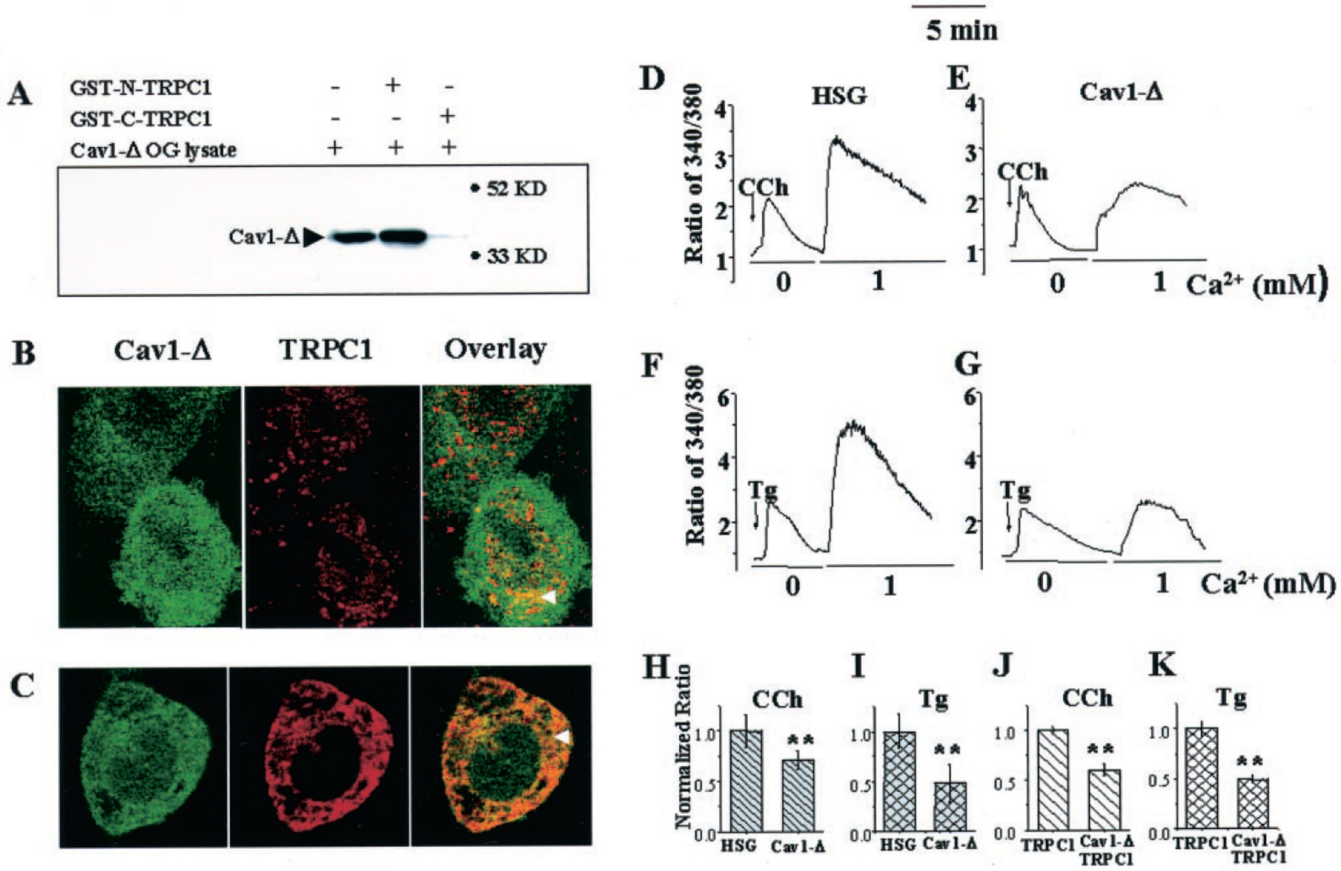

Fig. 5. Effect of mutant caveolin-1 on TRPC1 localization and SOCE

A, interaction of YFP-Cav1Δ51–169 with GST-N-TRPC1 and GST-C-TRPC1. *B* and *C*, localization of YFP-Cav1Δ51–169 (Cav1-Δ) and TRPC1 in HSG cells expressing Cav1-Δ. Cav1-Δ was detected by YFP fluorescence (*green* signal, *left panels* in *B* and *C*). Endogenous TRPC1 was detected using either anti-TRPC1 antibody (*B*), and exogenous TRPC1 (expressed using Ad-TRPC1) was detected with anti-HA antibody (*C*) and rhodamine-linked secondary antibody (*red* signal, *middle panels*). Colocalization of proteins is shown in overlays (*yellow* signal, *right panels*). Cells were imaged using a ×100 objective. *D–G*, fluorescence traces of control HSG cells (*D* and *F*), and HSG cells stably expressing YFP-Cav1Δ51–169 (*E* and *G*), stimulated with CCh (*D* and *E*) or Tg (*F* and *G*) in calcium-free buffer followed by the addition of 1 mM calcium. *H* and *I*, *bar graphs* showing the averages (between 100 and 200 cells for each set) of peak fluorescence increase caused by SOCE (second peak in traces *D–G*). *J* and *K*, *bar graphs* of similar data obtained with control HSG cells and cells stably expressing YFP-Cav1Δ51–169 after infection with Ad-TRPC1 (fluorescence traces are not shown). Values have been presented relative to that in control cells. Values significantly different from controls are marked by *asterisks* ($p < 0.02$).

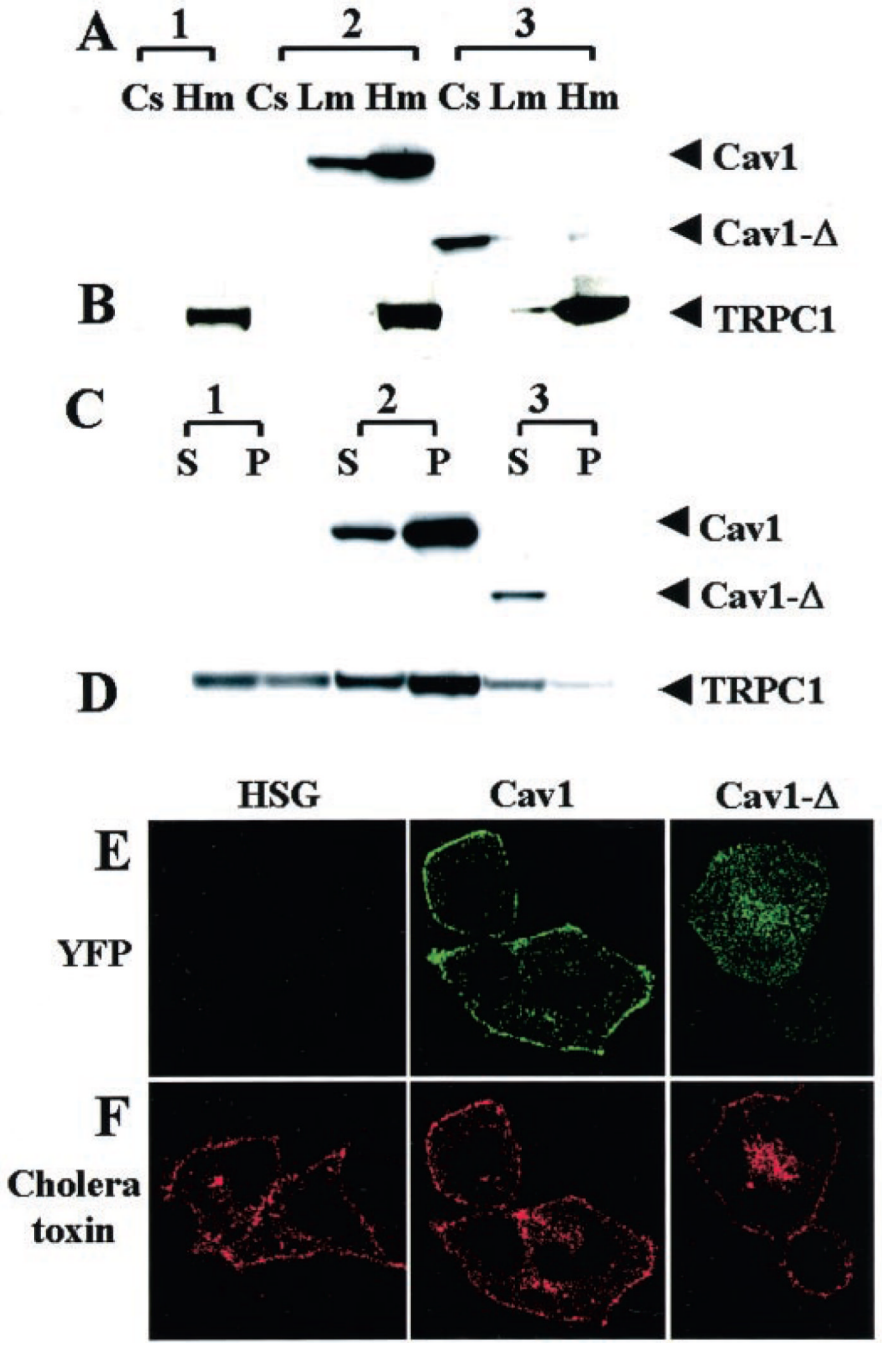

Fig. 6. Membrane interaction and detergent solubility of YFP-Cav1, YFP-Cav1Δ51–169, and HA-TRPC1

A and *B*, control HSG cells (*1*), HSG cells expressing YFP-Cav1 (*2*), or YFP-Cav1Δ51–169 (*3*) infected with Ad-TRPC1. Different subcellular fractions, cytosol (*Cs*), light membrane (*Lm*), and heavy membrane (*Hm*) were prepared as described under "Experimental Procedures." 20 μg of protein was loaded in each *lane*. Proteins were detected by Western blotting using either anti-YFP (*A*) or anti-HA (*B*) antibody. *C* and *D*, heavy membrane protein fraction (*Hm*) was prepared from each of the cell types described above and treated with Triton X-100 at 4 °C. The soluble (*S*) and insoluble (*P*) fractions were electrophoresed, and proteins were detected by Western blotting using either anti-YFP (*C*) or anti-HA

antibody (*D*). 30 μg of protein was loaded in each *lane*. *E* and *F*, detection of YFP (*E*, *green* signal) or cholera toxin 594 conjugate (*F*, *red* signal) in control HSG (*left panels*) and cells expressing YFP-Cav1 (*middle panels*) or YFP-Cav1Δ51–169 (*right panels*). Cells were imaged with a ×63 objective.